Available online at www.sciencedirect.com
SCIENCE DIRECT
Biochemical Pharmacology 69 (2005) 1667–1680
Biochemical Pharmacology
www.elsevier.com/locate/biochempharm

Prevention of hemorrhagic shock-induced lung injury by heme arginate treatment in rats

Kyoichiro Maeshima [a], Toru Takahashi [a,*], Kenji Uehara [a], Hiroko Shimizu [a], Emiko Omori [a], Masataka Yokoyama [a], Toru Tani [b], Reiko Akagi [c], Kiyoshi Morita [a]

[a] *Department of Anesthesiology and Resuscitology, Okayama University Medical School, 2-5-1 Shikata-cho, Okayama 700-8558, Japan*
[b] *Department of Surgery, Shiga University of Medical Science, Seta Tsukinowa-cho, Otsu, Shiga 520-2192, Japan*
[c] *Department of Nutritional Science, Okayama Prefectural University, 111 Kuboki, Soja, Okayama 719-1197, Japan*

Received 23 December 2004; accepted 9 March 2005

Abstract

Hemorrhagic shock followed by resuscitation (HSR) induces oxidative stress, which leads to acute lung injury. Heme oxygenase (HO)-1 (EC 1.14.99.3), the rate-limiting enzyme in heme catabolism, is inducible by oxidative stress and is thought to play an important role in the protection from oxidative tissue injuries. In this study, we examined expression of HO-1 as well as tissue injuries in the lung, liver, and kidney after HSR in rats. We also pretreated animals with heme arginate (HA), a strong inducer of HO-1, and examined its effect on the HSR-induced lung injury. HO-1 expression significantly increased in the liver and kidney following HSR, while its expression in the lung was very low and unchanged after HSR. In contrast to HO-1 expression, tissue injury and tumor necrosis factor-α (TNF-α) gene expression was more prominent in the lung compared with those in the liver and kidney. HA pretreatment markedly induced HO-1 in pulmonary epithelial cells, and ameliorated the lung injury induced by HSR as judged by the improvement of histological changes, while it decreased TNF-α and inducible nitric oxide synthase gene expression, lung wet weight to dry weight ratio, and myeloperoxidase activity. In contrast, inhibition of HO-1 by tin-mesoporphyrin administration abolished the beneficial effect of HA pretreatment. These findings suggest that tissues with higher HO-1 may be better protected than those with lower HO-1 from oxidative tissue injury induced by HSR. Our findings also indicate that HA pretreatment can significantly suppress the HSR-induced lung injury by virtue of its ability to induce HO-1.

Keywords: Acute lung injury; Heme arginate; Heme oxygenase-1; Hemorrhagic shock; Inflammation; Oxidative injury

1. Introduction

Hemorrhagic shock followed by resuscitation (HSR) induces a systemic inflammatory response that results in multiple organ impairment [1–3], including ALI, which is a major clinical problem, leading to significant mortality and morbidity [2,4]. Oxidative stress has been implicated as an important cause of its pathogenesis [3,5,6]. However, the suppression of oxidative stress has not been fully investigated in the strategic improvement of treatment for ALI [7,8]. Moreover, to our knowledge, there has been no report which compared the extent of lung injuries to that of other organs, such as the liver and the kidney, following HSR. HO-1, the rate-limiting enzyme in heme catabolism [9], is induced not only by its substrate heme [9] but also by various oxidative stresses [10], and is thought to confer protection to cells against oxidative injuries [11–13]. Several studies have demonstrated that overexpression of pulmonary HO-1 protects lung cells from oxidant injury in certain models of ALI [14–17]. However, the effect of HO-1 induction by agents available for clinical use has not been examined. Heme arginate (HA), which is a water-soluble and stable metabolite of the reaction of hemin and L-arginine [18], is known to strongly induce HO activity [19], and has been used for treatment of

Abbreviations: ALAS, δ-aminolevulinate synthase; ALI, acute lung injury; CO, carbon monoxide; HA, heme arginate; HO, heme oxygenase; HSR, hemorrhagic shock followed by resuscitation; iNOS, inducible nitric oxide synthase; IOD, integrated optical density; LPS, lipopolysaccharide; MAPK, mitogen-activated protein kinase; MPO, myeloperoxidase; SnMP, tin-mesoporphyrin; TNF-α, tumor necrosis factor-α; wet/dry, wet-weight to dry-weight

* Corresponding author. Tel.: +81 86 235 7327; fax: +81 86 231 0565.
E-mail address: takatoru@cc.okayama-u.ac.jp (T. Takahashi).

0006-2952/$ – see front matter © 2005 Elsevier Inc. All rights reserved.
doi:10.1016/j.bcp.2005.03.007

acute relapses of patients with acute hepatic porphyria [20,21]. In this study, we examined expression of HO-1 as well as tissue injuries in the lung, the liver, and the kidney after HSR in rats. We also pretreated animals with HA and examined its effect on the HSR-induced lung injury. We report here that HO-1 is markedly induced following HSR in the liver and the kidney, whereas HO-1 is not induced by the same treatment in the lung. In contrast, tissue injury and inflammation was more pronounced in the lung than in the liver and the kidney. HA pretreatment markedly induced HO-1 in the lung, and ameliorated the lung injury and inflammation induced by HSR. In contrast, inhibition of HO activity by SnMP, a specific competitive inhibitor of HO [22], abolished the beneficial effect of HA pretreatment. These findings suggest that tissues with higher HO-1 expression such as liver and kidney are better protected than those with lower HO-1 expression such as lung, from oxidative tissue injury induced by HSR. Our findings also indicate that HA pretreatment can significantly suppress lung injury induced by HSR by virtue of its ability to induce HO-1.

2. Materials and methods

2.1. Animals

Animal experiments were approved by the Animal Care Committee of Okayama University Medical School; care and handling of the animals were in accordance with National Institutes of Health guidelines. Male Sprague–Dawley rats weighing 350–400 g were purchased from Charles River. They were housed in a temperature-controlled (25 °C) room with alternating 12-h light/12-h dark cycles and were allowed free access to water and chow diet until the start of experiments.

2.2. Hemorrhagic shock protocol

Rats were anesthetized with intraperitoneal sodium pentobarbital (50 mg/kg) and then subjected to sham or hemorrhagic shock as described previously [23]. In brief, the left femoral artery and the left femoral vein were dissected out using aseptic techniques and cannulated with heparinized polyethylene tube. Catheters were inserted into the left femoral artery for measurement of blood pressure, and the left femoral vein for the induction of hemorrhage. Hemorrhage was initiated by bleeding the animal into a heparinized syringe (10 units/ml) over a period of 15 min to achieve a mean arterial blood pressure of 30 mmHg. This level of blood pressure (30 ± 5 mmHg) was maintained for 60 min by further blood withdrawal or by reinfusing the shed blood. At this point, animals were resuscitated over 15 min by first returning all shed blood, followed by administering sterile saline as necessary. The sham group underwent all instrumentation procedures, but blood was not collected. Animals were allowed to breathe spontaneously throughout the experiment. To maintain body temperature within physiological range, all procedures were made over the heating pad under continuous monitoring of rectal body temperature. Electrocardiography was also measured continuously.

2.3. Experimental design

To determine the relationship between tissue injury and HO-1 expression, rats were divided into the following three groups: HSR-treated animals (HSR group, $n = 24$), sham-operated animals (sham group, $n = 6$), and untreated control animals (untreated control group, $n = 3$). Next, to examine the effect of HA on HO-1 expression in the lung, rats were administered with various doses of HA (corresponding to 0–100 mg/kg of hemin) intravenously via tail vein (HA group, $n = 42$). HA solution (25 mg of hemin/ml) was prepared as described previously [18], immediately prior to use. Briefly, 15.3 mmol (2.67 g) of L-arginine was dissolved in 40 ml of water, and mixed with 10 g of ethanol and 40 g of 1,2-propanediol then water added to total volume of 100 ml followed by the addition of 3.83 mmol (2.5 g) of hemin. After stirring for 30 min, the solution was passed through a 0.45 μm filter (Millipore). Control rats received the same volume of the vehicle (153 mM L-arginine in 40% 1,2-propanediol and 10% ethanol solution) (Vehicle group, $n = 9$). Some rats were also administered with SnMP (0.5 μmol/kg; Frontier Scientific), a competitive inhibitor of HO activity [22], at 16 h after HA treatment (HA/SnMP group, $n = 6$). SnMP was prepared as described below, immediately before use. SnMP had been dissolved in a small volume of 0.1N NaOH solution, and then pH was adjusted to 7.6 with 0.01 M sodium phosphate buffer [24]. Finally, to test the effects of HA on HSR-induced lung injury, HSR rats were randomly assigned to the following four groups: control with sham operation (Control group, $n = 8$), pretreatment with vehicle (1,2-propanediol (40%) and ethanol (10%) solution) before HSR (Vehicle/HSR group, $n = 8$), pretreatment with HA before HSR (HA/HSR group, $n = 8$), and pretreatment with HA followed by SnMP administration before HSR treatment (HA/SnMP/HSR group, $n = 8$). HA (30 mg of hemin/kg) or the vehicle was injected at 18 h before HSR, and SnMP (0.5 μmol/kg) was injected at 2 h before HSR via tail vein, respectively. Under light anesthesia with ethyl ether, animals were sacrificed by decapitation at each defined time point (0–24 h). The tissues were excised and frozen immediately in liquid nitrogen and stored at −80 °C until use for the preparation of RNA and measurement of MPO activity. For the preparation of pulmonary microsomal fraction, animals were sacrificed by bleeding through a catheter in aorta under light anesthesia with ethyl ether and lungs were excised, and rinsed quickly and gently in physiologic saline.

2.4. cDNA probes

Template cDNA for HO-1 was rat pRHO-1 [25]. Template cDNA for TNF-α was rat TNF-α cDNA corresponding to 27–668 base pairs [26], which was cloned from LPS (*Escherichia coli*, 0128:B8; Sigma Chemical, 10 mg/kg, i.p.)-treated rat ileum library and constructed in pGEM-T Vector (Promega) [27]. Template cDNA for iNOS was rat iNOS cDNA corresponding to 1259–1714 bp [28], which was also cloned from the LPS-treated rat ileum library and constructed in the pGEM-T Vector [29]. All probes used for Northern blot analysis were [α-^{32}P]dCTP (NEN Life Science Products)-labeled cDNA probes prepared according to the manufacturer's instructions by using a random primer DNA labeling system (Amersham Pharmacia Biotech) [24].

2.5. RNA isolation and Northern blot analysis

Total RNA was isolated from the rat tissues using Tri-Reagent™ (Sigma Chemical) according to the manufacturer's protocol. Northern blotting was performed as described previously [24]. Twenty micrograms of total RNA were subjected to electrophoresis in a 1.2% (w/v) agarose gel containing 6.5% (v/v) formaldehyde. After blotting on a sheet of Bio-Rad Zeta-Probe membrane (Bio-Rad Laboratories), RNA samples were hybridized with [α-^{32}P]dCTP-labeled cDNA probe followed by washing under stringent conditions. The membrane was exposed to a sheet of Fuji Medical radiograph film with an intensifying screen at −70 °C, and autoradiographs were quantified by using an image scanner (GelPrint™ 2000i, Genomic Solutions) and a computerized image analysis software (Basic Quantifier™ Version 3.0, Genomic Solutions), which calculated IOD [24].

2.6. Western blot analysis

Lungs were homogenized in three volumes of 0.1 M potassium phosphate buffer (pH 7.4) containing 0.25 M sucrose and centrifuged at 10,000 × *g* for 30 min at 4 °C, followed by 104,000 × *g* centrifugation of the supernatant for 60 min at 4 °C, to obtain the microsomal fraction as a pellet. The pellet was resuspended in 0.02 M Tris–HCl (pH 7.4) containing 20% (v/v) glycerol and microsomal protein content was determined by the method of Lowry [30]. Western blotting was performed as described previously [24].

Samples equivalent to 50 μg of protein were applied to a 12% (w/v) polyacrylamide-SDS gel. After electrophoretic separation, proteins were transferred to Nitrocellulose membrane (Bio-Rad Laboratories). The membrane was blocked with Tris-buffered saline containing 10% (w/v) skim milk at 4 °C overnight, followed by incubation with a rabbit anti-HO-1 polyclonal antibody (StressGen Biotechnologies) diluted at 1:1000 with Tris-buffered saline containing 3% (w/v) skim milk. Then the membrane was treated with horseradish peroxidase-labeled goat anti-rabbit IgG (KPL). Antigen–antibody complexes were visualized with an ECL™ chemiluminescence system (Amersham Pharmacia Biotech) and short exposure of the membrane to X-ray films. The obtained signals were quantified as described above. The transfer efficiency and an equal amount of loading per lane were verified by staining nitrocellulose membranes using Amido Black solution [31].

2.7. Lung HO activity

Tissue was homogenized in three volumes of 0.05 M Tris–HCl (pH 7.8) containing 0.25 M sucrose, 20% (w/v) glycerol, 3 units/ml of heparin, and a protease inhibitor (Complete, Boehringer Mannheim GmbH), and centrifuged at 10,000 × *g* for 15 min at 4 °C. The supernatant was collected and centrifuged at 105,000 × *g* for 60 min at 4 °C. After centrifugation, the microsomal pellet was collected and resuspended in 20 mM Tris–HCl (pH 7.4) containing 1.15% KCl and a protease inhibitor and used to measure HO activity spectrophotometrically as described previously [24,32]. The cytosolic fraction prepared from the liver of adult untreated rats served as a source of biliverdin reductase in the HO assay. HO activity was expressed as picomoles of bilirubin formed per milligram of protein per 60 min. Protein concentration was determined by the method of Lowry [30].

2.8. Histological study

For histological examination, the tissue was fixed in 10% neutral buffered formalin, embedded in paraffin, and sectioned at 4–6 μm thickness. After deparaffinization and dehydration, the sections were stained with hematoxylin and eosin for microscopic examination. For immunohistochemical examination, the enzymatic activity of endogenous peroxidases in the tissue section was first blocked with 3% hydrogen peroxide, followed by incubation with rabbit polyclonal anti-rat HO-1 (StressGen Biotechnologies) at 37 °C for 3 h. The antigen–antibody reaction was detected using a secondary anti-rabbit antibody and an avidin–biotin immunoperoxidase staining kit (DAKO) [33]. The positive reaction was visualized as brown stain following treatment with 3,3′-diaminobenzidine. Normal rabbit serum was used as control for non-specific staining. Sections were counterstained with hematoxylin.

2.9. Lung wet/dry ratio

Lung tissue samples were blotted, weighed, and then dried at 110 °C for 24 h. The dry tissue weight was then determined and wet/dry ratios were calculated as an index of pulmonary edema [34].

2.10. Lung MPO assay

Lung MPO activity was measured as described by Bradley et al. [35], with some modification. Briefly, tissue was homogenized in 50 mM potassium phosphate buffer (pH 6.0) containing 0.5% (w/v) hexadecyltrimethylammonium bromide (Nacalai Tesque Co.) followed by the centrifugation at 15,000 × *g* for 15 min at 4 °C. After centrifugation, 0.1 ml of the supernatant was mixed with 2.9 ml of 50 mM potassium phosphate buffer (pH 6.0) containing 0.167 mg/ml *o*-dianisidine dehydrochloride (Sigma Chemical). Following the addition of 5 μl of 0.3% hydrogen peroxide to the mixture, the increase in color was monitored at 460 nm for 1 min on a Spectrophotometer (U-3000™ HITACHI). The protein concentration of the supernatant was determined by the method of Lowry [30]. Values are reported as change in O.D. (ΔO.D.) per milligram of protein.

2.11. Statistical analysis

Statistical evaluation was performed with analysis of variance followed by Scheffé's *F*-test, by using Statview software (Abacus Concepts). Differences were considered as significant at $p < 0.05$. Data are presented as mean ± S.D.

3. Results

3.1. Time courses of TNF-α mRNA expression and histological changes after HSR

Although it is well-known that tissue inflammation after HSR is prominent not only in the lung but also in the liver [2,3], there has been no report which compared the extent of tissue inflammation in various organs following HSR. Thus, we examined time course changes in the level of

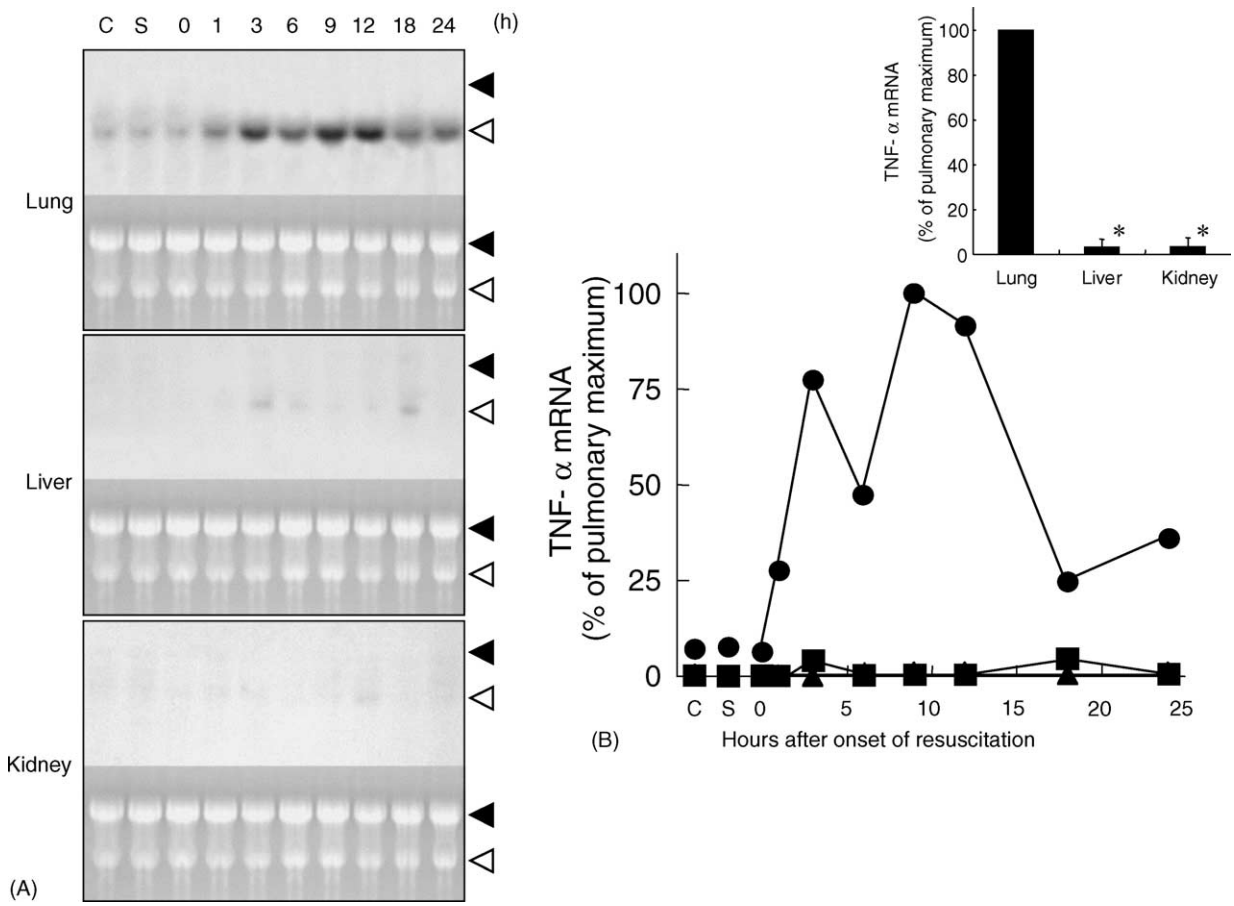

Fig. 1. Effect of HSR on TNF-α gene expression in the lung, liver, and kidney. Rats were killed at 0, 1, 3, 6, 9, 12, 18, and 24 h after HSR. Lungs, livers, and kidneys were excised for Northern blot analysis as described in Section 2. (A) Twenty micrograms of total RNA was subjected to Northern blot analysis. Shown are the autoradiographic signals of RNA blot hybridized with [α-^{32}P]dCTP-labeled TNF-α cDNA. Ethidium bromide staining of the same RNA is shown as a loading control. Filled arrowhead, 28S ribosomal RNA; open arrowhead, 18S ribosomal RNA; C, untreated control; S, sham-operated animals. Three independent experiments showed similar results, and a typical example is shown. (B) Levels of TNF-α mRNA are expressed as the percentage of the maximal level of pulmonary TNF-α mRNA. (●) Lung, (■) liver, and (▲) kidney. *Inset:* maximal levels of TNF-α mRNA after HSR in the lung, liver, and kidney are expressed as the percentage of the maximal level of pulmonary TNF-α mRNA. Data are presented as mean ± S.D. ($n = 3$). Statistical analysis by analysis of variance with Scheffé's *F*-test. $^{*}p < 0.05$ vs. lung.

TNF-α mRNA in the lung, the liver, and the kidney. TNF-α mRNA was barely detectable in all tissues both in untreated control animals (0.18 ± 0.10 IOD, $n = 3$) and sham-operated animals (0.20 ± 0.12 IOD, $n = 3$). Following HSR, TNF-α mRNA level in the lung significantly increased at 3 h (0.97 ± 0.23 IOD, $n = 3$), decreased transiently at 6 h (0.60 ± 0.13 IOD, $n = 3$), and then increased and reached a maximum at 9 h (1.26 ± 0.32 IOD, $n = 3$), followed by the gradual decrease (Fig. 1) [36]. In contrast to the lung, TNF-α mRNA was hardly detectable in the liver and the kidney throughout the course of observational period (Fig. 1). When the maximal levels of TNF-α mRNA in each tissue of three independent experiments were compared, the level in the lung (1.26 ± 0.32 IOD, $n = 3$) was almost 20 times higher than that of the liver (0.04 ± 0.04 IOD, $n = 3$, $p < 0.05$ versus lung) and the kidney (0.04 ± 0.05 IOD, $n = 3$, $p < 0.05$ versus lung) (Fig. 1B, inset). Histological examination revealed that lungs from rats after HSR showed a significant tissue injury, as judged by alveolar septal thickening with marked infiltration of inflammatory cells (Fig. 2B). In contrast to the lung, apparent cellular injuries were not observed in the liver and the kidney (Fig. 2D and F).

3.2. Time courses of HO-1 mRNA expression and immunohistochemical demonstration of HO-1 after HSR

Since some recent papers reported that HO-1 is induced by oxidative stress including ischemia/reperfusion in various tissues [11], we examined the level of HO-1 mRNA in the lung, the liver and the kidney after HSR. HO-1 mRNA was only barely detectable in all tissues examined both in untreated control and in sham-operated animals (Fig. 3). Following HSR, HO-1 mRNA level in the liver significantly increased at 3 h, reached a maximum at 6 h, and then rapidly declined to control level by 9 h (Fig. 3) [37]. In the kidney, its level abruptly increased and reached a maximum at 3 h after HSR, followed by a rapid decrease to the basal level by 6 h (Fig. 3). In contrast, HO-1 mRNA was only barely detectable in the lung before and after HSR (Fig. 3). When the maximally induced levels of HO-1 mRNA after HSR of three independent experiments were compared, the levels in the liver and in the kidney were almost 20 times and more than 40 times larger than that in the lung, respectively (liver, 37.80 ± 19.01 IOD, or kidney, 83.34 ± 6.96, $p < 0.05$ versus lung, 1.90 ± 3.00; $n = 3$ for each group) (Fig. 3B, inset). Immunohistochemical analysis revealed that HO-1-positive cells were not observed in the kidney or in the lung of sham-operated control animals (Fig. 4A and E), while in the liver of control animals, some HO-1 staining was observed marginally in non-parenchymal cells (Fig. 4C) [37]. Consistent with enhanced HO-1 gene expression in the liver, at 12 h after HSR, positive staining of HO-1 protein was observed not only in non-parenchymal cells, but also in parenchymal hepatocytes around the central vein [37], the cells that are known to be the target of ischemia/reperfusion injury (Fig. 4D) [38]. Similarly, in the kidney of HSR rats, positive staining of HO-1 protein was also observed in the tubular epithelial cells (Fig. 4F), the target cells in renal

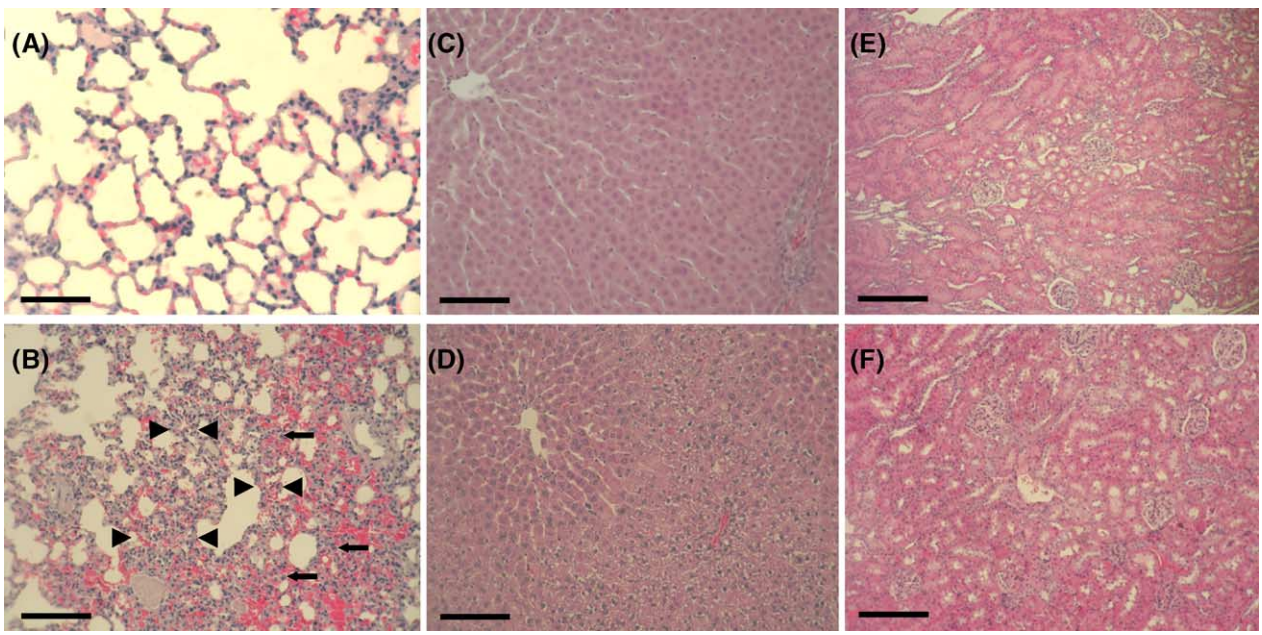

Fig. 2. Histological changes in the lung, liver, and kidney after HSR. Rats subjected to HSR were killed at 12 h after the treatment. Lungs, livers, and kidneys were removed for histological examination as described in Section 2. Three independent experiments showed similar results, and a typical example is shown. (A) Lung, (C) liver, and (E) kidney from sham-operated control animals. (B) Lung, (D) liver, and (F) kidney from HSR animals. Pulmonary alveolar septal thickening and infiltration of inflammatory cells were typically observed at the portion indicated by arrowheads and arrows, respectively, although these findings were observed throughout the field. The bars represent 100 μm. Sections were stained with hematoxylin and eosin.

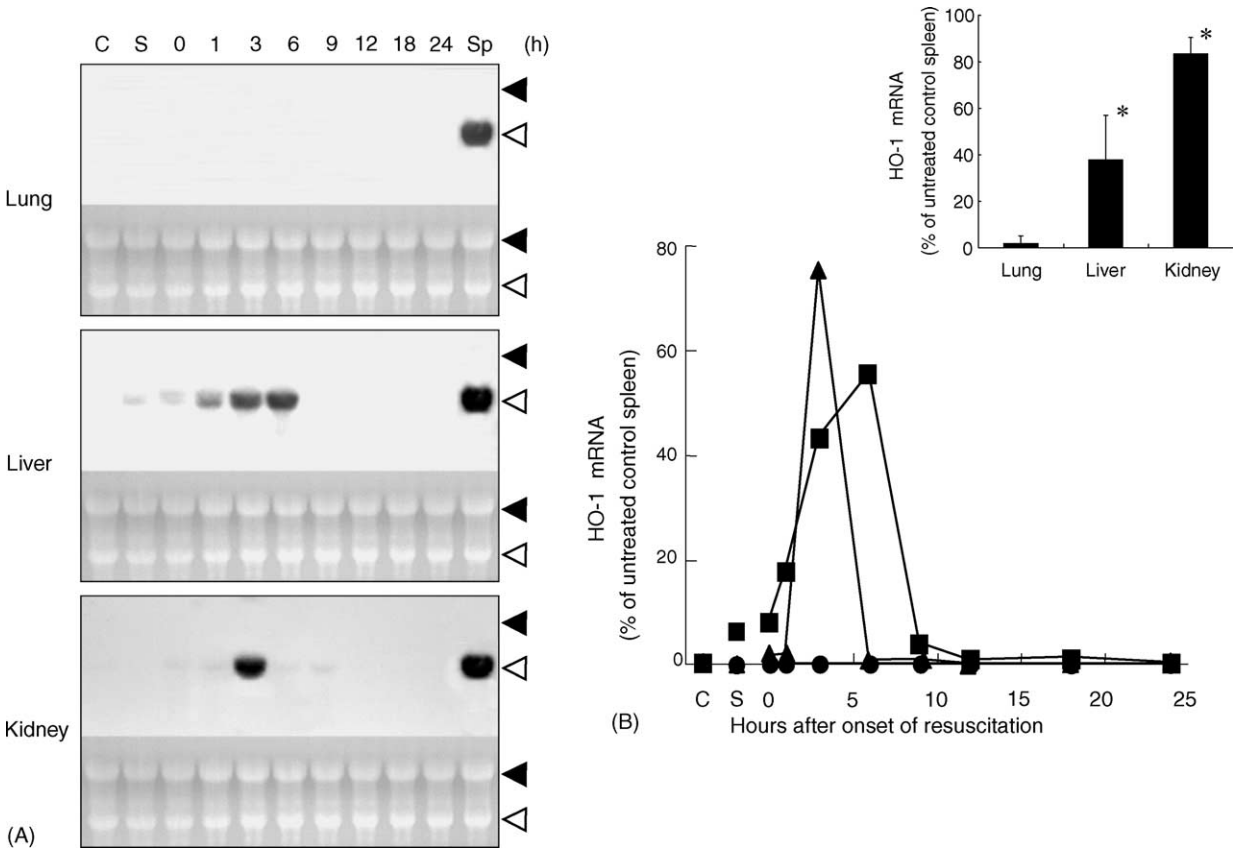

Fig. 3. Effect of HSR on HO-1 gene expression in the lung, liver, and kidney. Rats were killed at 0, 1, 3, 6, 9, 12, 18, and 24 h after HSR. Lungs, livers, and kidneys were excised for Northern blot analysis as described in Section 2. (A) Twenty micrograms of total RNA was subjected to Northern blot analysis. Shown are the autoradiographic signals of RNA blot hybridized with [α-^{32}P]dCTP-labeled HO-1 cDNA. Ethidium bromide staining of the same RNA is shown as a loading control. Filled arrowhead, 28S ribosomal RNA; open arrowhead, 18S ribosomal RNA; C, untreated control; S, sham-operated animals; Sp, untreated control spleen. Three independent experiments showed similar results, and a typical example is shown. (B) Levels of HO-1 mRNA are expressed as the percentage of the level of HO-1 mRNA in untreated control spleen. (●) Lung, (■) liver, and (▲) kidney. *Inset:* maximal levels of HO-1 mRNA after HSR in the lung, liver, and kidney are expressed as the percentage of the level of HO-1 mRNA in untreated control spleen. Data are presented as mean ± S.D. ($n = 3$). Statistical analysis by analysis of variance with Scheffé's F-test. $^{*}p < 0.05$ vs. lung.

ischemia/reperfusion injury [39,40]. Sections of the liver and the kidney from HSR rats showed no signal when treated with non-immune rabbit serum (data not shown). In contrast to the liver and the kidney, HO-1 protein expression was only barely detectable in the lung of untreated and HSR-treated rats (Fig. 4B).

3.3. Effect of HA administration on HO-1 expression

As shown thus far, tissue injury and inflammation was more prominent in the lung than those in the liver and the kidney, while HO-1 was markedly expressed in the liver and the kidney as compared with that of the lung. Namely, there is a clear reciprocal relationship between tissue injuries and inflammation, and HO-1 expression, suggesting that tissues with marked HO-1 expression such as liver and kidney are better protected than tissues with lesser HO-1 expression such as lung. Therefore, we examined whether induction of HO-1 by pharmacological treatment may protect lungs from HSR-induced injury. Since HA is a strong inducer of HO-1 in the liver and the kidney [19], we examined whether HA administration induces HO-1 expression in the lung. While HO-1 mRNA was hardly detectable in vehicle-treated control animals, pulmonary HO-1 mRNA levels increased 6 h after the treatment in a dose-dependent manner. The maximal level (100 mg of hemin/kg) of HO-1 mRNA was ~3-fold to that of untreated control spleen, in which HO-1 is known to be constitutively expressed and the highest among various tissues examined in untreated animals [41] (Fig. 5A). Although the maximal effect of HA on HO-1 mRNA expression was observed at a dose of 100 mg of hemin/kg in HA, doses greater than 60 mg of hemin/kg in HA were also associated with ascites. Thus, we used 30 mg of hemin/kg in HA in the following experiments. HA-treated animals (30 mg of hemin/kg) showed normal histological appearance in the lung (Fig. 6B, bottom inset) without any hepatorenal toxicity (data not shown). We then examined time course changes in the level of pulmonary HO-1 mRNA following HA (30 mg of hemin/kg) treatment. While pulmonary HO-1 mRNA was barely detectable in the vehicle-treated control rats, its level increased markedly and reached a maximum at 6 h after HA administration, the level of which was almost the same as that of untreated control spleen, and

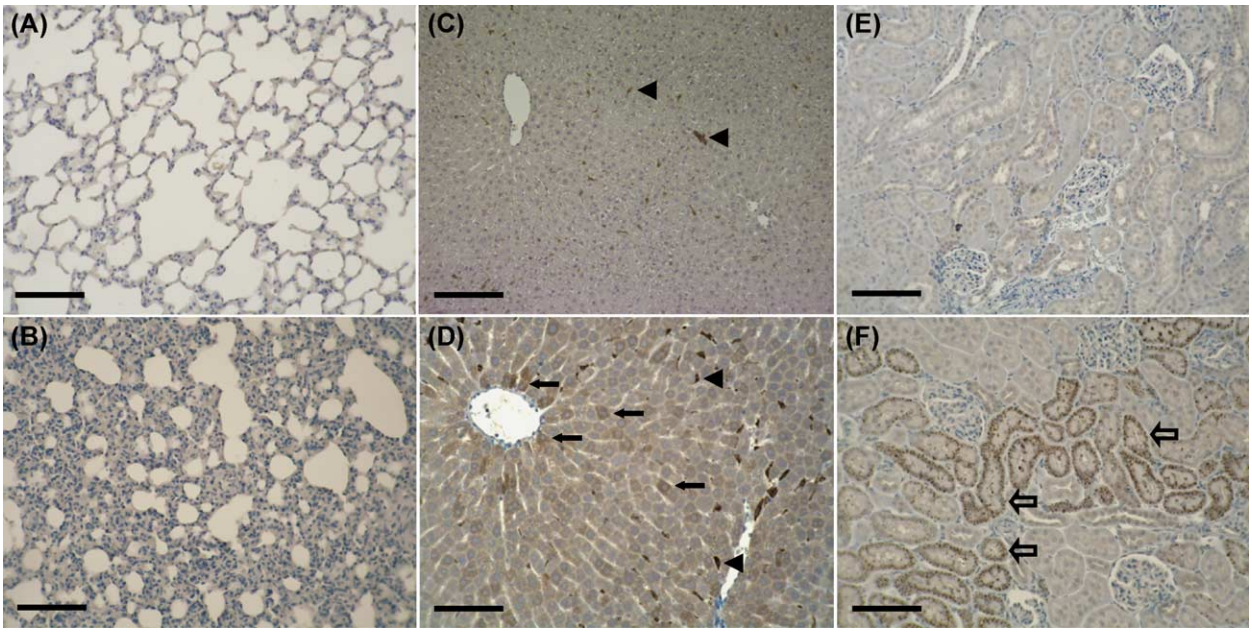

Fig. 4. Immunohistochemistry of HO-1 in the lung, liver, and kidney after HSR. Sections from 12 h after HSR were used for immunohistochemical detection of HO-1, by using rabbit polyclonal anti-rat HO-1 antibody as a primary antibody. Immunohistochemical staining was carried out as described in Section 2. Each photograph is the representative of at least three independent experiments. (A) Lung, (C) liver, and (E) kidney from sham-operated control animals. (B) Lung, (D) liver, and (F) kidney from HSR animals. Arrowheads, black arrows, and open arrows indicate HO-1 positively stained Kupffer cells, hepatocytes, and renal tubular epithelial cells, respectively. The bars represent 100 μm.

then declined gradually to the control level by 24 h (Fig. 5B). We also examined the level of HO-1 protein by Western blot analysis after HA administration. While pulmonary HO-1 protein was slightly detectable in the control animals (0.28 ± 0.03 IOD), its level started to increase at 12 h after the treatment (0.55 ± 0.07 IOD), and reached a maximum at 18 h (0.72 ± 0.10 IOD), and then this high level is maintained by 24 h (0.70 ± 0.06 IOD) (Fig. 6A). Thus, we decided to administer HA 18 h before HSR in subsequent experiments. We also carried out immunohistochemical analysis of HO-1 in the lung from rats at 18 h after HA treatment, to determine what type of cells in the lung expressed HO-1. In the lung of vehicle-treated control rats, there was no positive staining of HO-1 protein. In contrast, marked HO-1 protein expression was observed after HA administration in the pulmonary epithelial cells, the target cells of ALI [42] (Fig. 6B). Certain synthetic heme analogues, such as tin protoporphyrin and cobalt protoporphyrin, were reported to possess the ability to simultaneously inhibit as well as induce the enzyme HO-1 in the liver [43]. Thus, to confirm whether our finding on the increase in pulmonary HO-1 mRNA and protein expression is reflected in HO activity, we examined the level of HO activity in the lung following treatment with HA. Pulmonary HO activity increased by ∼2.5-fold compared with the control concentration at 18 h after the treatment (Vehicle group, 38.37 ± 13.08 pmol bilirubin/60 min/mg protein versus HA group, 103.46 ± 34.13; $n = 6$ for each group, $p < 0.05$) (Fig. 7), and this increase was entirely abolished by following administration of SnMP, a competitive inhibitor of HO activity [22] (HA/SnMP group, 48.10 ± 22.90, $n = 6$, $p < 0.05$ versus HA group) (Fig. 7), indicating that induced pulmonary HO-1 activity is also vulnerable to inhibition by SnMP, as is the case with HO-1 in the liver and the kidney [24,39].

3.4. Effect of HA pretreatment on TNF-α and iNOS gene expression after HSR

Since HA administration markedly induced functional HO-1 protein in the pulmonary epithelial cells, the target cells in ALI [42], we administered HA prior to HSR and examined its effect on lung inflammation caused by HSR. Pulmonary TNF-α mRNA was barely detectable in sham-operated control animals (0.22 ± 0.14 IOD, $n = 3$) (Fig. 8A), while it increased significantly in Vehicle/HSR animals 3 h after HSR (Vehicle/HSR group, 1.18 ± 0.23 IOD, $p < 0.05$ versus Control group) (Fig. 8A). In contrast, its level in HA/HSR animals markedly decreased by ∼50% of the level of Vehicle/HSR animals (HA/HSR group, 0.55 ± 0.12 IOD, $p < 0.05$ versus Vehicle/HSR group) (Fig. 8A). We also examined the effect of HA pretreatment on iNOS gene expression in the lung. Similar to changes in TNF-α gene expression, 3 h after HSR, pulmonary iNOS mRNA level significantly increased in Vehicle/HSR animals whereas its level in sham-operated control animals remained hardly detectable (Control group, 0.00 ± 0.00 IOD versus Vehicle/HSR group, 0.60 ± 0.10, $p < 0.05$) (Fig. 8B) [44]. In contrast, its level in HA/HSR animals markedly decreased by ∼30% of the level in Vehicle/HSR animals (HA/HSR group, 0.20 ± 0.07 IOD, $p < 0.05$ versus Vehicle/HSR group) (Fig. 8B). Thus, HSR-induced

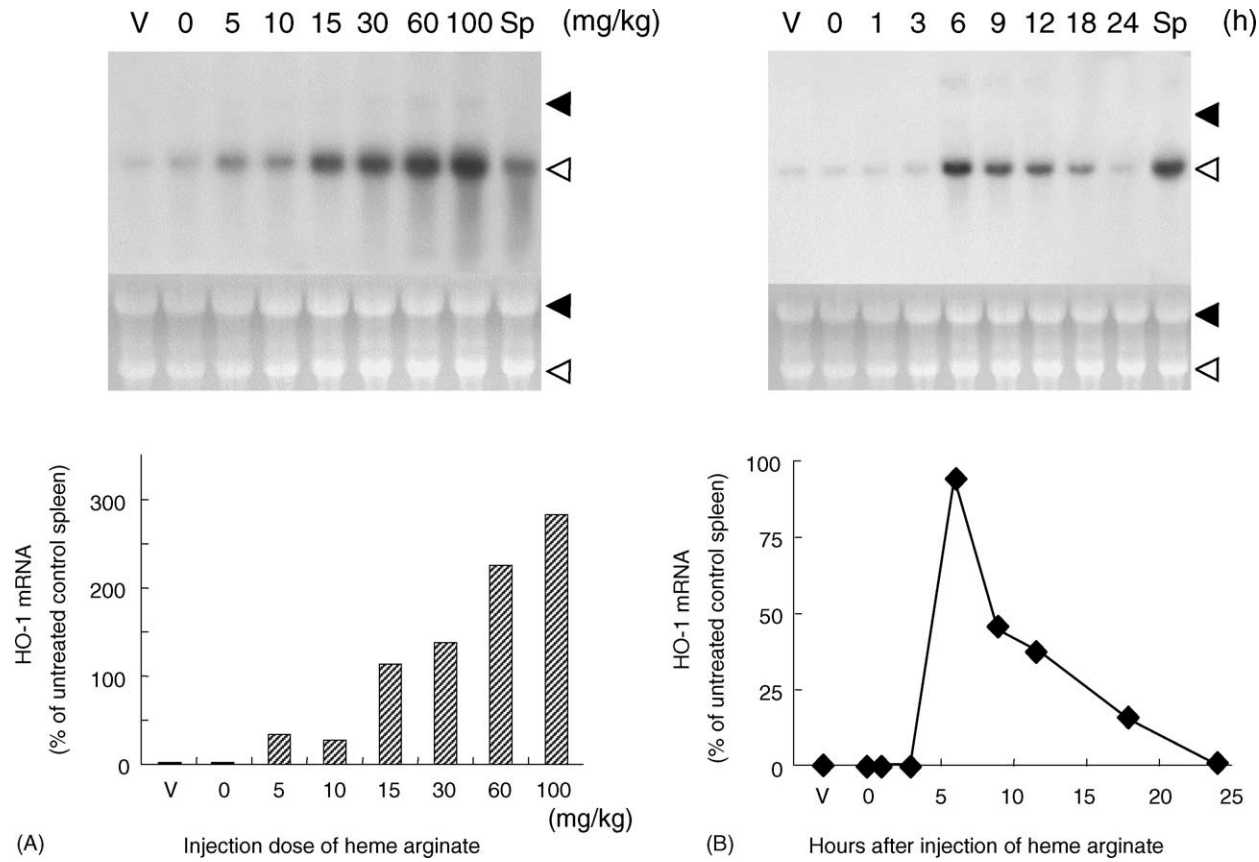

Fig. 5. Effect of HA administration on HO-1 gene expression in the rat lung. (A) Dose–response relationship of pulmonary HO-1 gene expression after HA administration. Rats injected intravenously with HA at doses of 0, 5, 10, 15, 30, 60, and 100 mg of hemin/kg or vehicle, the volume of which was identical to that of 100 mg of hemin/kg in HA solution, were killed at 6 h after the injection. Lungs were removed for Northern blot analysis. (B) Time course of pulmonary HO-1 gene expression after HA treatment. Rats injected intravenously with HA (30 mg of hemin/kg) were killed at 0, 1, 3, 6, 9, 12, 18, and 24 h after the injection. Vehicle-treated rats were also killed at 6 h after the injection. Lungs were removed for Northern blot analysis. *Top:* 20 μg of total RNA was subjected to Northern blot analysis. Shown are the autoradiographic signals of RNA blot hybridized with [α-^{32}P]dCTP-labeled HO-1 cDNA. Ethidium bromide staining of the same RNA is shown as a loading control. Filled arrowhead, 28S ribosomal RNA; open arrowhead, 18S ribosomal RNA; V, vehicle-treated control animal; Sp, untreated control spleen. Three independent experiments showed similar results, and a typical example is shown. *Bottom:* levels of HO-1 mRNA are expressed as the percentage of the level of HO-1 mRNA in untreated control spleen.

pulmonary inflammation was markedly attenuated by HA pretreatment. To examine whether the beneficial effect of HA pretreatment on tissue inflammation is mediated by HO activity, we administered SnMP, a specific competitive inhibitor of HO [22], intravenously 2 h before HSR to HA-pretreated animals (HA/SnMP/HSR animals), and examined its effect on TNF-α and iNOS gene expression. TNF-α mRNA level in HA/SnMP/HSR animals was elevated and reached a similar level as observed in Vehicle/HSR animals (HA/SnMP/HSR group, 1.35 ± 0.18 IOD, $p < 0.05$ versus HA/HSR group) (Fig. 8A). Similarly, iNOS mRNA level in HA/SnMP/HSR animals was also markedly increased compared to that of HA/HSR animals (HA/SnMP/HSR group, 0.45 ± 0.06 IOD, $p < 0.05$ versus HA/HSR group) (Fig. 8B). Thus, SnMP administration to HA-pretreated animals essentially abolished the protective effect of HA pretreatment. All these findings indicate that HA-induced HO activity alleviates HSR-induced pulmonary inflammation, while inhibition of HO activity aggravates this process, indicating the critical protective role of HO-1 in the HSR-induced pulmonary inflammation.

3.5. Effect of HA pretreatment on histological changes, wet/dry ratio, and MPO activity of the lung after HSR

Next we examined the effect of HA pretreatment on lung injury after HSR. Lung injury was assessed by morphological examination, lung wet/dry ratio as an index of pulmonary edema [34], and lung MPO activity as a measure of pulmonary neutrophil content [45]. Sections of the lung excised from sham-operated control animals were essentially normal (Fig. 9A). In contrast, Vehicle/HSR animals showed pronounced alveolar septal thickening with marked infiltration of inflammatory cells at 12 h after HSR (Fig. 9B). Consistent with the histological findings, lung wet/dry ratio (Control group, 4.90 ± 0.05 versus Vehicle/HSR group, 5.10 ± 0.10, $p < 0.05$) (Fig. 10A) as well as lung MPO activity (Control group, 0.38 ± 0.10 Δ absorbance/mg protein versus Vehicle/HSR group, 1.00 ± 0.12, $p < 0.05$) 12 h after HSR were significantly increased compared with that of the sham-operated control animals (Fig. 10B) [44,46,47]. In contrast, HA pretreatment greatly suppressed lung injury as revealed by

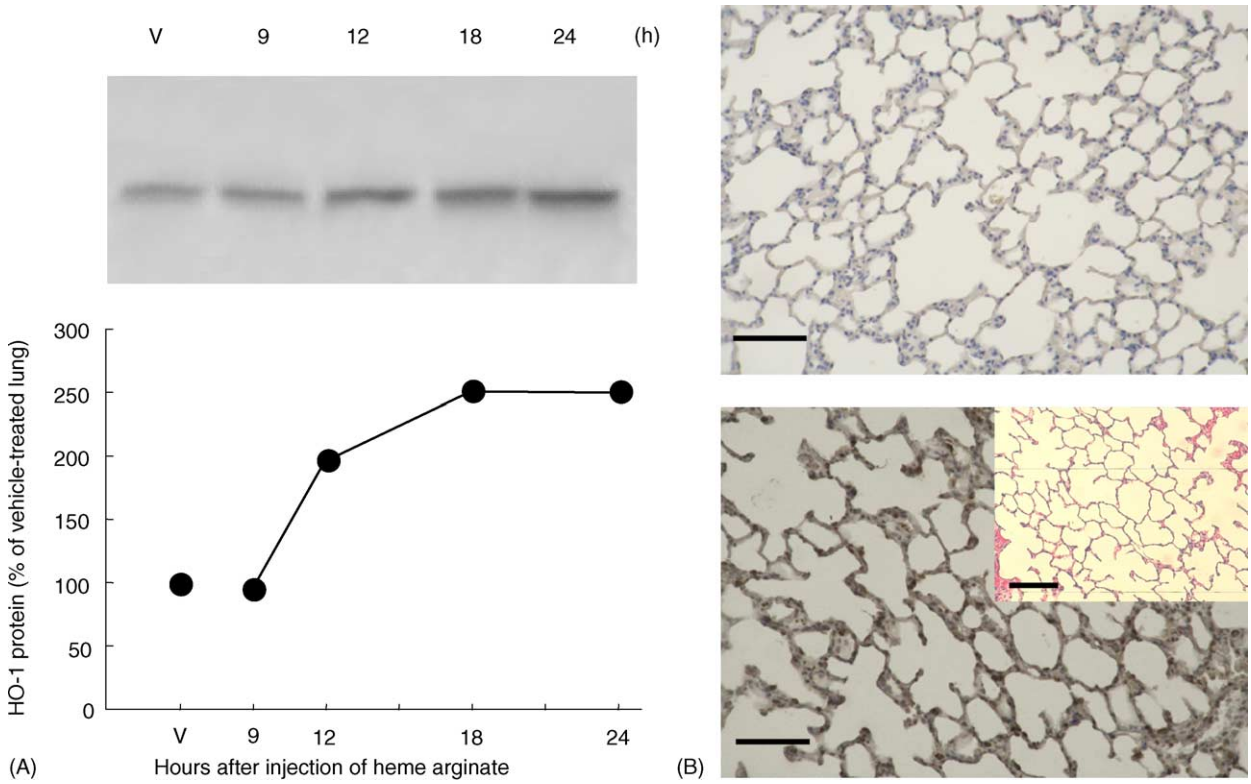

Fig. 6. Effect of HA administration on HO-1 protein expression in the rat lung. (A) *Top:* rats injected intravenously with HA (30 mg of hemin/kg) or vehicle were killed at 9, 12, 18, and 24 h after the injection. Lungs were removed for Western blot analysis as described in Section 2. Shown are the chemiluminescent signals of protein blots reacted with a rabbit polyclonal anti-rat HO-1 antibody. Three independent experiments showed similar results, and a typical example is shown. V, vehicle-treated control animal. *Bottom:* levels of HO-1 protein are expressed as the percentage of the level of HO-1 protein in vehicle-treated control lung. (B) Immunohistochemistry of HO-1 in the lung of HA administered rats. Lung sections from rats 18 h after the injection intravenously with HA (30 mg of hemin/kg) or vehicle were used for immunohistochemical detection of HO-1 by using rabbit polyclonal anti-rat HO-1 as a primary antibody. Immunohistochemical staining was carried out as described in Section 2. Each photograph represents at least three independent experiments. *Top:* vehicle-treated control lung; *bottom:* HSR lung; *inset:* hematoxylin eosin stained lung section from 12 h after HA administration. The bars represent 100 μm.

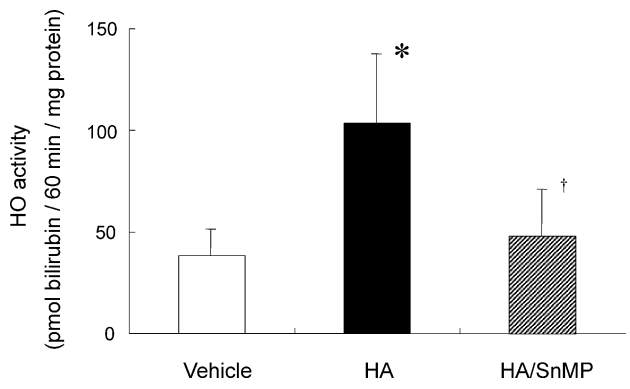

Fig. 7. Effect of HA administration on HO activity in the rat lung. Rats were injected intravenously with HA (30 mg of hemin/kg) or vehicle via tail vein. Some rats were additionally administered with SnMP (0.5 μmol/kg) intravenously 16 h after HA administration, i.e., 2 h prior to HSR. The lung was removed at 18 h after HA or vehicle administration, and HO activity was measured as described in Section 2. Vehicle, vehicle-treated control animals; HA, HA-administered animals; HA/SnMP, HA administration followed by SnMP. Data are presented as mean ± S.D. ($n = 6$ for each group). Statistical analysis by analysis of variance with Scheffé's F-test. $^{*}p < 0.05$ vs. Vehicle; $^{\dagger}p < 0.05$ vs. HA.

lesser histological damage (Fig. 9C), marked decrease in lung wet/dry ratio (HA/HSR group, 4.86 ± 0.06, $p < 0.05$ versus Vehicle/HSR group), which reached to almost the same level as sham-operated control animals (HA/HSR group versus Control group, $p = 0.443$) (Fig. 10A), and significant reduction in MPO activity (HA/HSR group, 0.73 ± 0.13, $p < 0.05$ versus Vehicle/HSR group) (Fig. 10B). To examine whether the amelioration of lung injury by HA pretreatment is attributable to increased HO activity, HA-pretreated animals were also treated with SnMP. Sections from HA/SnMP/HSR animals revealed exacerbation of lung injuries comparable to that observed in Vehicle/HSR animals (Fig. 9B and D). SnMP administration to HA-pretreated animals also significantly increased not only lung wet/dry ratio (HA/SnMP/HSR group, 5.15 ± 0.08, $p < 0.05$ versus HA/HSR group) but also lung MPO activity (HA/SnMP/HSR group, 1.04 ± 0.01, $p < 0.05$ versus HA/HSR group) to a level comparable to that in untreated HSR animals (Fig. 10). Thus, SnMP administration ablated the improvement of lung injury by HA pretreatment via inhibition of HO activity. All these findings corroborate to the fact that

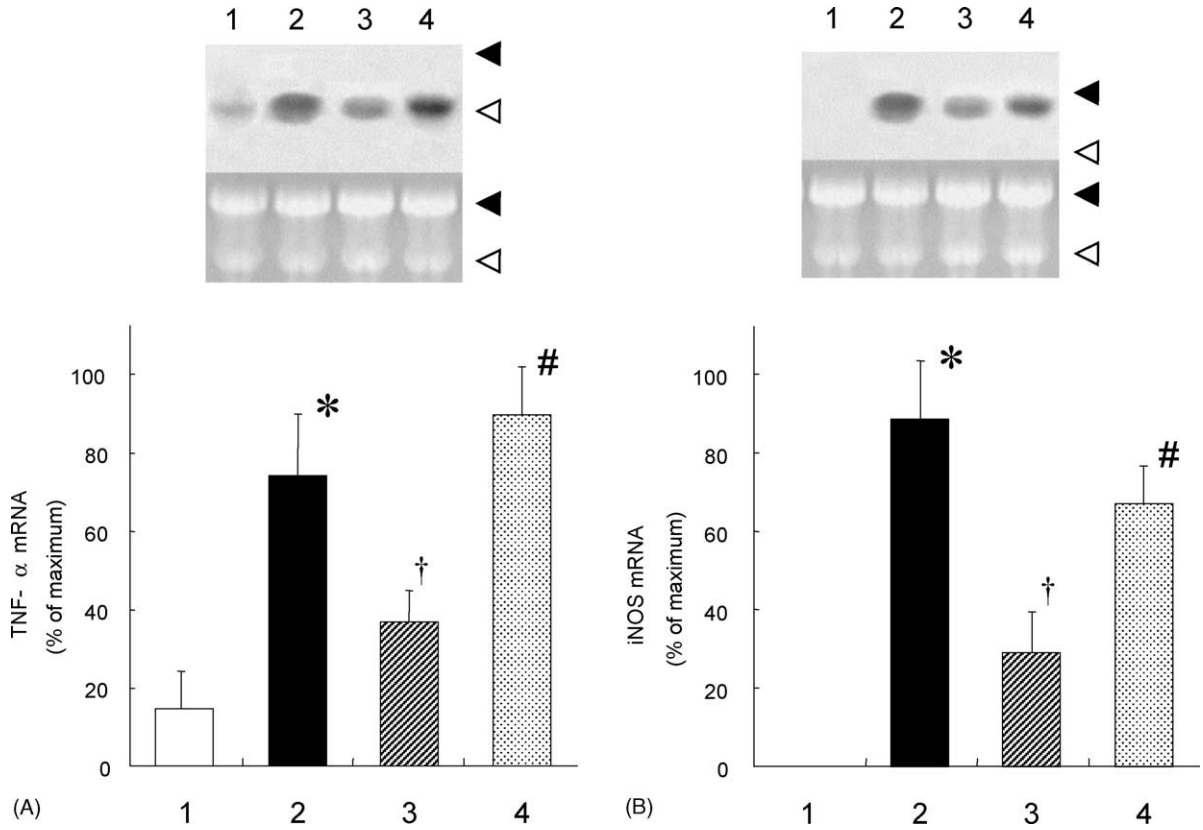

Fig. 8. Effect of HA pretreatment on gene expression of pulmonary TNF-α and iNOS after HSR. HA (30 mg of hemin/kg) or vehicle was administered to rats intravenously 18 h before HSR. SnMP (0.5 μmol/kg) was administered to rats intravenously 2 h before HSR. Lungs were excised 3 h after HSR for Northern blot analysis as described in Section 2. *Top:* 20 μg of total RNA was subjected to Northern blot analysis. Shown are the autoradiographic signals of RNA blot hybridized with [α-^{32}P]dCTP-labeled TNF-α (A) or iNOS (B) cDNA. Ethidium bromide staining of the same RNA is shown as a loading control. Filled arrowhead, 28S ribosomal RNA; open arrowhead, 18S ribosomal RNA. Three independent experiments showed similar results, and a typical example is shown. Lane 1: sham-operated control; lane 2: HSR with vehicle pretreatment; lane 3: HSR with HA pretreatment; lane 4: HSR with HA pretreatment followed by SnMP administration. *Bottom:* levels of TNF-α (A) or iNOS (B) mRNA are expressed as the percentage of its maximal level. Lane numbers correspond to numbers in top panel. Data are presented as mean ± S.D. ($n = 3$ for each group). Statistical analysis by analysis of variance with Scheffé's F-test. $^{*}p < 0.05$ vs. Control; $^{\dagger}p < 0.05$ vs. HSR with Vehicle; $^{\#}p < 0.05$ vs. HSR with HA.

amelioration of the HSR-induced lung injury by HA pretreatment is accomplished by the induction of HO-1 activity.

4. Discussion

Our present study demonstrated that HO-1 mRNA and protein were markedly induced in the liver and the kidney in rats, while its expression remained barely detectable in the lung after HSR. In contrast to HO-1 expression, tissue injury and inflammation were more prominent in the lung compared with those in the liver and kidney. To our knowledge, this is the first report, which demonstrated the protective effect of HA pretreatment on HSR-induced lung injury. Our data also show that the protective effect of HA treatment was due to its ability to induce HO-1 in pulmonary epithelial cells. Inhibition of HO activity by SnMP, a specific competitive inhibitor of the enzyme, entirely abolished the beneficial effects of HA pretreatment, indicating that HO-1 plays an important role in protecting lung cells from oxidative injury caused by HSR.

In the liver, HO-1 mRNA level markedly increased at 3 h, reaching a maximum at 6 h followed by a rapid decrease to the control level by 9 h (Fig. 3) [37]. In the kidney, there was a transient but marked increase in HO-1 mRNA level at 3 h after HSR (Fig. 3). As noted earlier, its level in the lung was hardly detectable prior to HSR and did not increase in response to HSR (Fig. 3). Thus, HO-1 gene expression was markedly tissue-specific. Tissue-specific HO-1 gene expression was also observed in a rat model of sepsis produced by intraperitoneal injection of LPS, which also causes oxidative tissue injury [48]. Tamion et al. previously reported that pulmonary HO-1 mRNA expression was significantly increased after HSR using the same model as ours [46]. However, they did not compare the level of HO-1 gene expression in the lung to the levels in other tissues such as liver and kidney, thus it was unclear whether pulmonary HO-1 mRNA induction was greater than those in liver and kidney.

Consistent with the marked induction of HO-1 mRNA in the liver and the kidney, HO-1 protein expression was also markedly increased in hepatocytes in the liver [37] as well

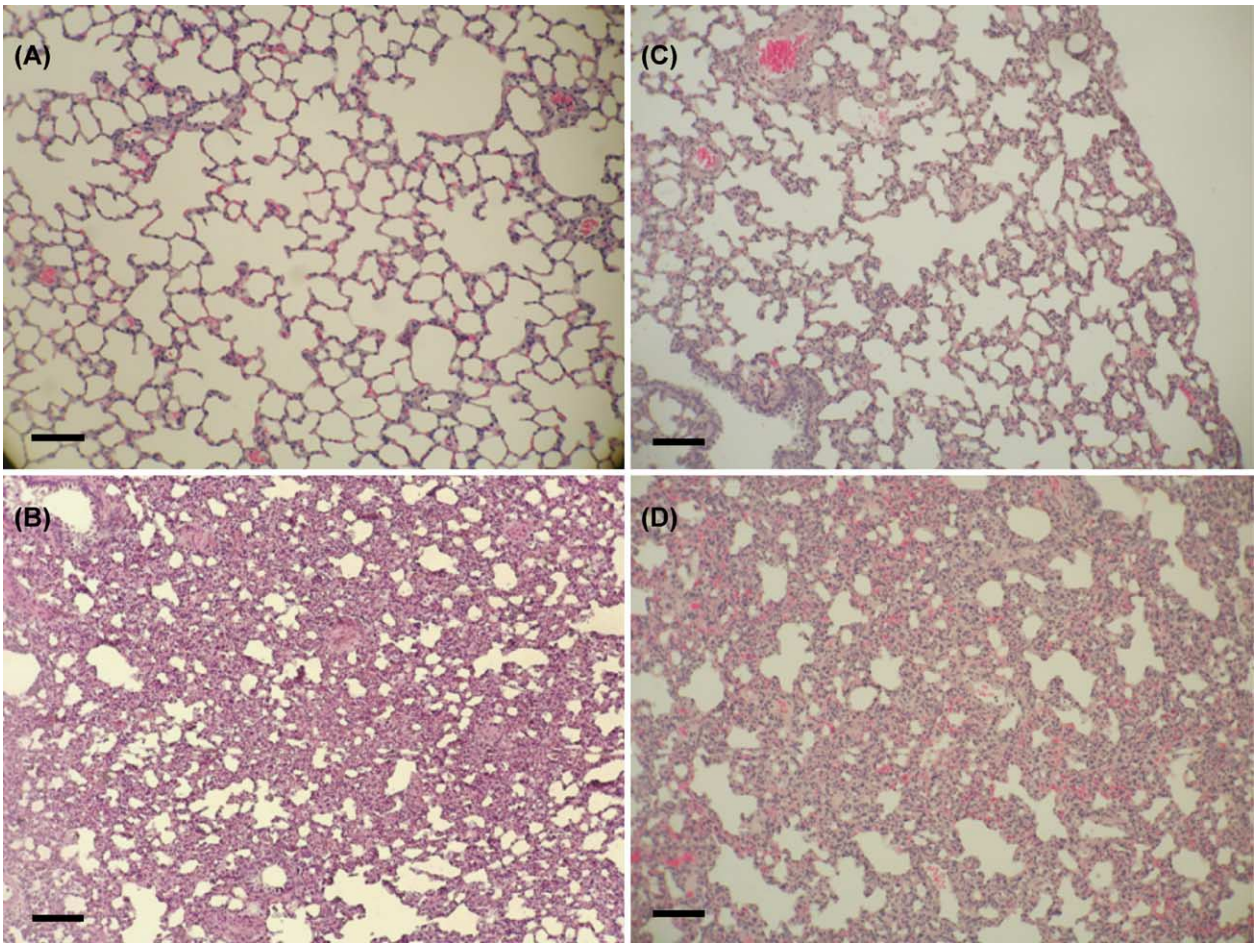

Fig. 9. Effect of HA pretreatment on histological changes of the lung after HSR. HA (30 mg of hemin/kg) or vehicle was administered to rats intravenously 18 h before HSR. SnMP (0.5 μmol/kg) was administered to rats intravenously 2 h before HSR. Twelve hours after HSR, lungs were excised, and fixed in formalin and stained with hematoxylin and eosin as described in Section 2. Each photograph is the representative of at least three independent experiments. (A) Sham-operated control; (B) HSR with vehicle pretreatment; (C) HSR with HA pretreatment; (D) HSR with HA pretreatment followed by SnMP administration. The bars represent 100 μm.

as in tubular epithelial cells in the kidney (Fig. 4), both of which are the target cells of ischemia/reperfusion injury [38,40]. In contrast to HO-1 expression, tissue injury was more prominent in the lung where HO-1 expression and induction was negligible (Fig. 2). TNF-α mRNA levels, a molecular marker of inflammation, were also much higher in the lung than in the liver and the kidney following HSR (Fig. 1). A similar situation was also previously observed in the intestinal tissue injury in a rat model of sepsis produced by intraperitoneal injection of LPS [27], in which HO-1 was markedly increased in the upper intestine, such as duodenum and jejunum, while its expression was barely detectable in the lower intestine, such as ileum and colon. In contrast, tissue injury and inflammation was more prominent in the lower intestine than those in the upper intestine. Moreover, inhibition of HO activity in the upper intestine exacerbated its tissue injury and inflammation. Thus, both in the intestine and in the lung, there is a clear reciprocal relationship between HO-1 expression and tissue injury, strongly suggesting a protective role of HO-1 against oxidative tissue injury [11]. In support of our hypothesis, HA pretreatment, which markedly induces functional HO-1 protein in pulmonary epithelial cells (Figs. 6 and 7), markedly ameliorated lung inflammation after HSR, shown by decreases in gene expression of TNF-α as well as iNOS (Fig. 8). Consistent with the decrease in inflammatory gene expression by HA pretreatment, histological examination showed significantly ameliorated tissue injuries of the lung compared with those of untreated rats, as revealed by the decrease in alveolar septal thickening due to interstitial edema with reduced infiltration of inflammatory cells, as confirmed by the decrease in lung wet/dry ratio and MPO activity, respectively (Figs. 9 and 10). Furthermore, the administration of SnMP, a specific competitive inhibitor of HO activity, to HA-pretreated animals abolished the beneficial effect of HA on HSR-induced tissue injury and inflammation of the lung (Figs. 8–10), indicating that protective effects of HA treatment on lung injury after HSR are attributable to its ability to increase HO activity by HO-1 induction in the pulmonary epithelial cells.

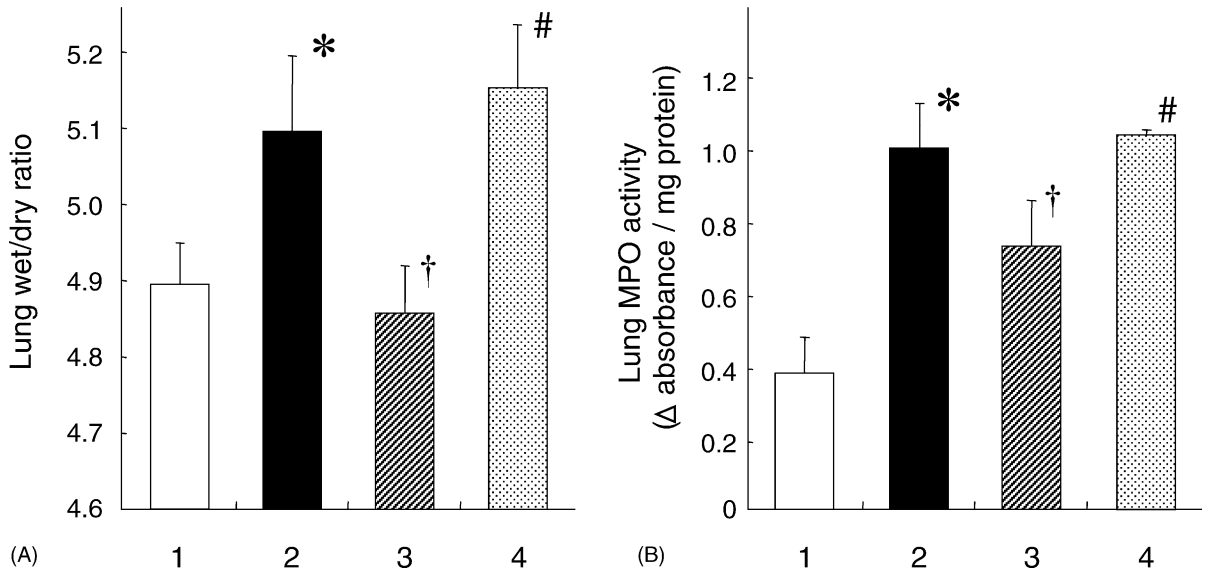

Fig. 10. Effect of HA pretreatment on lung wet/dry ratio and lung MPO activity after HSR. HA (30 mg of hemin/kg) or vehicle was administered to rats intravenously 18 h before HSR. SnMP (0.5 μmol/kg) was administered to rats intravenously 2 h before HSR. Lungs were excised at 12 h after HSR and lung wet/dry ratio (A) and lung MPO activity (B) were measured as described in Section 2. Data are presented as mean ± S.D. ($n = 5$ for each group). Lane 1: sham-operated control; lane 2: HSR with vehicle pretreatment; lane 3: HSR with HA pretreatment; lane 4: HSR with HA pretreatment followed by SnMP administration. Statistical analysis by analysis of variance with Scheffé's F-test. $^{*}p < 0.05$ vs. Control; $^{\dagger}p < 0.05$ vs. HSR with vehicle; $^{\#}p < 0.05$ vs. HSR with HA.

It has previously been reported that beneficial effects of HO-1 induction were observed in the experimental model of ALI [14–17]. We have also previously reported that pharmacological induction of HO-1 confers protection against oxidative tissue injuries in various model systems such as halothane-induced hepatic injury [33] and ischemic acute renal failure [39]. However, the significance of HO-1 induction by clinically used agents has not been examined. HA has been used as a drug for treatment of acute relapses of patients with acute hepatic porphyria [20,21]. It has also been reported that HA administration strongly induces HO-1 in the liver and the kidney in rats [19]. In this study, we demonstrated that HA administration induced HO-1 mRNA in the lung in a time- and dose-dependent manner (Fig. 5). Consistent with augmented HO-1 gene expression, the intense HO-1 protein expression was observed in the pulmonary epithelial cells, the target cells in ALI [42], in HA-treated animals, which showed almost normal unaffected histology (Fig. 6). As expected, the lung of HA-pretreated rats had a marked elevation of HO activity (Fig. 7). These results indicate that HA treatment induces functional HO-1 protein in pulmonary epithelial cells without notable adverse effects. As noted earlier, HO-1 induced by HA treatment almost completely relieved of severe lung injury caused by HSR, suggesting the possibility of its clinical application as an inducer of HO-1 for the treatment of ALI.

The rationale for the use of HA in the treatment of patients with acute hepatic porphyria is its ability to inhibit ALAS, the rate-limiting enzyme in heme biosynthesis [49], activity [20,21]. As it is extremely difficult to detect ALAS activity in non-hepatic and non-erythroid cells, such as lung, we examined non-specific ALAS (ALASl) mRNA [50] levels in the lung of rats treated with HA. Following HA treatment, ALASl mRNA levels showed an initial rise at 3 h (∼1.6-fold compared to vehicle-treated control), remained at this level for 3 h, then rapidly declined and reached to a minimum level by 9 h (45% of the control), and returned almost to the basal level at 12 h and remained at that level thereafter (data not shown) [51]. As animals were subjected to HSR 18 h following HA treatment, it appears that ALAS1 may not be involved in the protection of lung injury in a significant manner.

In addition to HO-1, it has been reported that HO-2, a constitutive form of HO isozymes [41], plays an important role in the defense against oxidative lung injury. HO-2 deficient mice have been reported to be more susceptible to hyperoxic lung damage than wild-type mice despite the fact that HO-1 protein level is twice higher in the lung of HO-2 deficient mice than that in wild-type mice [52]. Moreover, Adachi et al. have reported that HO-2 deficient mice also reveal hypoxemia with normal arterial CO_2 tension and intact alveolar architecture, suggesting that HO-2 is also responsible for the ventilation–perfusion matching that optimizes oxygenation of pulmonary blood [53].

The mechanism by which HO-1 mediates protection against HSR-induced tissue injury is not yet entirely clear. However, it appears to involve at least mitigation of reactive oxygen species formation that is known to play a critical role in HSR-induced tissue injury [3,5,6]. In this respect, it is worth reviewing the HO-catalyzed reaction. HO-1 oxidatively cleaves heme, and yields CO, iron, and

biliverdin IXα, which is then reduced to bilirubin IXα by bilirubin reductase [9]. Although an excess amount of free iron can be cytotoxic as it can catalyze Fenton reaction [54], iron produced by HO in the cell is immediately inactivated by sequestration into ferritin [55]. In addition, biliverdin IXα and bilirubin IXα function as potent endogenous anti-oxidants [56]. Bilirubin IXα can also be converted to biliverdin IXα, leading to an accelerated anti-oxidant cycle that could amplify the anti-oxidant effect of biliverdin or bilirubin alone [57]. CO is also known to exhibit anti-inflammatory and anti-apoptotic functions, which are thought to be mediated, at least in part, by the activation of p38 MAPK signaling pathway [58,59]. Very recently, it has also been reported that the anti-apoptotic effect of CO involves inhibition of Fas/FasL expression, and other apoptosis-related factors including caspases, mitochondrial cytochrome *c* release, Bcl-2 proteins and poly (ADP-ribose) polymerase cleavage in addition to activation of p38α MAPK isoform and its upstream MAPK (MKK3) [60]. Thus, CO may also have an important protective function against apoptosis induced by oxidative tissue injuries. Accordingly, induction of HO-1 results not only in the reduction of oxidant stress by removing free heme, a potent pro-oxidant [61], but also in the increase in the level of anti-oxidants, and in the suppression of apoptosis. While it is unclear to what extent each mechanism may contribute, these findings may be all important in the host cellular defense against oxidative tissue injuries.

Acknowledgments

We are grateful to Dr. Shigeki Shibahara (Tohoku University, Sendai, Japan) for providing us with pRHO-1. We are also grateful to Dr. Shigeru Sassa (the Rockefeller University, NY) for reviewing our manuscript.

References

[1] Regel G, Grotz M, Weltner T, Sturm JA, Tscherne H. Pattern of organ failure following severe trauma. World J Surg 1996;20:422–9.
[2] Bhatia M, Moochhala S. Role of inflammatory mediators in the pathophysiology of acute respiratory distress syndrome. J Pathol 2004;202:145–56.
[3] Jarrar D, Chaudry IH, Wang P. Organ dysfunction following hemorrhage and sepsis: mechanisms and therapeutic approaches. Int J Mol Med 1999;4:575–83 [Review].
[4] Hudson LD, Milberg JA, Anardi D, Maunder RJ. Clinical risks for development of the acute respiratory distress syndrome. Am J Respir Crit Care Med 1995;151:293–301.
[5] Fink MP. Reactive oxygen species as mediators of organ dysfunction caused by sepsis, acute respiratory distress syndrome, or hemorrhagic shock: potential benefits of resuscitation with Ringer's ethyl pyruvate solution. Curr Opin Clin Nutr Metab Care 2002;5:167–74.
[6] Szabo C. The pathophysiological role of peroxynitrite in shock, inflammation, and ischemia-reperfusion injury. Shock 1996;6:79–88.
[7] Wiedemann HP, Arroliga AC, Komara Jr JJ. Emerging systemic pharmacologic approaches in acute respiratory distress syndrome. Respir Care Clin N Am 2003;9:419–35.
[8] Vincent JL. New management strategies in ARDS. Immunomodulation Crit Care Clin 2002;l8:69–78.
[9] Shibahara S. Regulation of heme oxygenase gene expression. Semin Hematol 1988;25:370–6.
[10] Ryter SW, Choi AM. Heme oxygenase-1: molecular mechanisms of gene expression in oxygen-related stress. Antioxid Redox Signal 2002;4:625–32.
[11] Takahashi T, Morita K, Akagi R, Sassa S. Heme oxygenase-1: a novel therapeutic target in oxidative tissue injuries. Curr Med Chem 2004;11:1545–61.
[12] Takahashi T, Morita K, Akagi R, Sassa S. Protective role of heme oxygenase-1 in renal ischemia. Antioxid Redox Signal 2004;6: 867–77.
[13] Otterbein LE, Choi AM. Heme oxygenase: colors of defense against cellular stress. Am J Physiol Lung Cell Mol Physiol 2000;279:L1029–37.
[14] Ito K, Ozasa H, Kojima N, Miura M, Iwa T, Senoo H, et al. Pharmacological preconditioning protects lung injury induced by intestinal ischemia/reperfusion in rat. Shock 2003;19:462–8.
[15] Otterbein LE, Kolls JK, Mantell LL, Cook JL, Alam J, Choi AM. Exogenous administration of heme oxygenase-1 by gene transfer provides protection against hyperoxia-induced lung injury. J Clin Invest 1999;103:1047–54.
[16] Taylor JL, Carraway MS, Piantadosi CA. Lung-specific induction of heme oxygenase-1 and hyperoxic lung injury. Am J Physiol 1998;274:L582–90.
[17] Otterbein L, Sylvester SL, Choi AM. Hemoglobin provides protection against lethal endotoxemia in rats: the role of heme oxygenase-1. Am J Respir Cell Mol Biol 1995;13:595–601.
[18] Tenhunen R, Tokola O, Linden IB. Haem arginate: a new stable haem compound. J Pharm Pharmacol 1987;39:780–6.
[19] Levere RD, Martasek P, Escalante B, Schwartzman ML, Abraham NG. Effect of heme arginate administration on blood pressure in spontaneously hypertensive rats. J Clin Invest 1990;86:213–9.
[20] Herrick AL, McColl KE, Moore MR, Cook A, Goldberg A. Controlled trial of haem arginate in acute hepatic porphyria. Lancet 1989;1: 1295–7.
[21] Tenhunen R, Mustajoki P. Acute porphyria: treatment with heme. Semin Liver Dis 1998;18:53–5.
[22] Valaes T, Petmezaki S, Henschke C, Drummond GS, Kappas A. Control of jaundice in preterm newborns by an inhibitor of bilirubin production: studies with tin-mesoporphyrin. Pediatrics 1994;93: 1–11.
[23] Tani T, Fujino M, Hanasawa K, Shimizu T, Endo Y, Kodama M. Bacterial translocation and tumor necrosis factor-alpha gene expression in experimental hemorrhagic shock. Crit Care Med 2000;28: 3705–9.
[24] Nakahira K, Takahashi T, Shimizu H, Maeshima K, Uehara K, Fujii H, et al. Protective role of heme oxygenase-1 induction in carbon tetrachloride-induced hepatotoxicity. Biochem Pharmacol 2003;66: 1091–105.
[25] Shibahara S, Muller R, Taguchi H, Yoshida T. Cloning and expression of cDNA for rat heme oxygenase. Proc Natl Acad Sci USA 1985;82: 7865–9.
[26] Estler HC, Grewe M, Gaussling R, Pavlovic M, Decker K. Rat tumor necrosis factor-alpha. Transcription in rat Kupffer cells and in vitro posttranslational processing based on a PCR-derived cDNA. Biol Chem Hoppe Seyler 1992;373:271–81.
[27] Fujii H, Takahashi T, Nakahira K, Uehara K, Shimizu H, Matsumi M, et al. Protective role of heme oxygenase-1 in the intestinal tissue injury in an experimental model of sepsis. Crit Care Med 2003;31: 893–902.
[28] Karlsen AE, Andersen HU, Vissing H, Larsen PM, Fey SJ, Cuartero BG, et al. Cloning and expression of cytokine-inducible nitric oxide

synthase cDNA from rat islets of Langerhans. Diabetes 1995;44:753–8.
[29] Maeshima K, Takahashi T, Nakahira K, Shimizu H, Fujii H, Katayama H, et al. A protective role of interleukin 11 on hepatic injury in acute endotoxemia. Shock 2004;21:134–8.
[30] Lowry O. Protein measurement with the folin phenol reagent. J Biol Chem 1951;193:265–75.
[31] Schaffner W, Weissmann C. A rapid, sensitive, and specific method for the determination of protein in dilute solution. Anal Biochem 1973;56:502–14.
[32] Tenhunen R, Marver HS, Schmid R. The enzymatic conversion of heme to bilirubin by microsomal heme oxygenase. Proc Natl Acad Sci USA 1968;61:748–55.
[33] Odaka Y, Takahashi T, Yamasaki A, Suzuki T, Fujiwara T, Yamada T, et al. Prevention of halothane-induced hepatotoxicity by hemin pretreatment: protective role of heme oxygenase-1 induction. Biochem Pharmacol 2000;59:871–80.
[34] Stephens KE, Ishizaka A, Larrick JW, Raffin TA. Tumor necrosis factor causes increased pulmonary permeability and edema. Comparison to septic acute lung injury. Am Rev Respir Dis 1988;137:1364–70.
[35] Bradley PP, Priebat DA, Christensen RD, Rothstein G. Measurement of cutaneous inflammation: estimation of neutrophil content with an enzyme marker. J Invest Dermatol 1982;78:206–9.
[36] Schwartz MD, Repine JE, Abraham E. Xanthine oxidase-derived oxygen radicals increase lung cytokine expression in mice subjected to hemorrhagic shock. Am J Respir Cell Mol Biol 1995;12:434–40.
[37] Rensing H, Bauer I, Datene V, Patau C, Pannen BH, Bauer M. Differential expression pattern of heme oxygenase-1/heat shock protein 32 and nitric oxide synthase-II and their impact on liver injury in a rat model of hemorrhage and resuscitation. Crit Care Med 1999;27:2766–75.
[38] Schon MR, Kollmar O, Akkoc N, Matthes M, Wolf S, Schrem H, et al. Cold ischemia affects sinusoidal endothelial cells while warm ischemia affects hepatocytes in liver transplantation. Transplant Proc 1998;30:2318–20.
[39] Toda N, Takahashi T, Mizobuchi S, Fujii H, Nakahira K, Takahashi S, et al. Tin chloride pretreatment prevents renal injury in rats with ischemic acute renal failure. Crit Care Med 2002;30:1512–22.
[40] Ratych RE, Bulkley GB. Free-radical-mediated postischemic reperfusion injury in the kidney. J Free Radic Biol Med 1986;2:311–9.
[41] Maines MD. Heme oxygenase: function, multiplicity, regulatory mechanisms, and clinical applications. FASEB J 1988;2:2557–68.
[42] Ware LB, Matthay MA. The acute respiratory distress syndrome. N Engl J Med 2000;342:1334–49.
[43] Sardana MK, Kappas A. Dual control mechanism for heme oxygenase: tin(IV)-protoporphyrin potently inhibits enzyme activity while markedly increasing content of enzyme protein in liver.. Proc Natl Acad Sci USA 1987;84:2464–8.
[44] Hierholzer C, Harbrecht B, Menezes JM, Kane J, MacMicking J, Nathan CF, et al. Essential role of induced nitric oxide in the initiation of the inflammatory response after hemorrhagic shock. J Exp Med 1998;187:917–28.
[45] Goldblum SE, Wu KM, Jay M. Lung myeloperoxidase as a measure of pulmonary leukostasis in rabbits. J Appl Physiol 1985;59:1978–85.
[46] Tamion F, Richard V, Bonmarchand G, Leroy J, Lebreton JP, Thuillez C. Induction of heme-oxygenase-1 prevents the systemic responses to hemorrhagic shock. Am J Respir Crit Care Med 2001;164:1933–8.
[47] Bahrami S, Yao YM, Leichtfried G, Redl H, Schlag G, Di Padova FE. Monoclonal antibody to endotoxin attenuates hemorrhage-induced lung injury and mortality in rats. Crit Care Med 1997;25:1030–6.
[48] Suzuki T, Takahashi T, Yamasaki A, Fujiwara T, Hirakawa M, Akagi R. Tissue-specific gene expression of heme oxygenase-1 (HO-1) and non-specific delta-aminolevulinate synthase (ALAS-N) in a rat model of septic multiple organ dysfunction syndrome. Biochem Pharmacol 2000;60:275–83.
[49] Granick S, Urata G. Increase in activity of delta-aminolevulinic acid synthetase in liver mitochondria induced by feeding of 3,5-dicarbethoxy-l,4-dihydrocollidine. J Biol Chem 1963;238:821–7.
[50] Yamamoto M, Kure S, Engel JD, Hiraga K. Structure, turnover, and heme-mediated suppression of the level of mRNA encoding rat liver delta-aminolevulinate synthase. J Biol Chem 1988;263:15973–9.
[51] Schacter BA, Yoda B, Israels LG. Cyclic oscillations in rat hepatic heme oxygenase and delta-aminolevulinic acid synthetase following intravenous heme administration. Arch Biochem Biophys 1976;173:11–7.
[52] Dennery PA, Spitz DR, Yang G, Tatarov A, Lee CS, Shegog ML, et al. Oxygen toxicity and iron accumulation in the lungs of mice lacking heme oxygenase-2. J Clin Invest 1998;101:1001–11.
[53] Adachi T, Ishikawa K, Hida W, Matsumoto H, Masuda T, Date F, et al. Hypoxemia and blunted hypoxic ventilatory responses in mice lacking heme oxygenase-2. Biochem Biophys Res Commun 2004;320:514–22.
[54] McCord JM. Iron, free radicals, and oxidative injury. Semin Hematol 1998;35:5–12.
[55] Vogt BA, Alam J, Croatt AJ, Vercellotti GM, Nath KA. Acquired resistance to acute oxidative stress. Possible role of heme oxygenase and ferritin. Lab Invest 1995;72:474–83.
[56] Stocker R, Yamamoto Y, McDonagh AF, Glazer AN, Ames BN. Bilirubin is an antioxidant of possible physiological importance. Science 1987;235:1043–6.
[57] Baranano DE, Rao M, Ferris CD, Snyder SH. Biliverdin reductase: a major physiologic cytoprotectant. Proc Natl Acad Sci USA 2002;99:16093–8.
[58] Brouard S, Otterbein LE, Anrather J, Tobiasch E, Bach FH, Choi AM, et al. Carbon monoxide generated by heme oxygenase 1 suppresses endothelial cell apoptosis. J Exp Med 2000;192:1015–26.
[59] Otterbein LE, Bach FH, Alam J, Soares M, Tao Lu H, Wysk M, et al. Carbon monoxide has anti-inflammatory effects involving the mitogen-activated protein kinase pathway. Nat Med 2000;6:422–8.
[60] Zhang X, Shan P, Alam J, Davis RJ, Flavell RA, Lee PJ. Carbon monoxide modulates Fas/Fas ligand, caspases, and Bcl-2 family proteins via the p38alpha mitogen-activated protein kinase pathway during ischemia-reperfusion lung injury. J Biol Chem 2003;278:22061–70.
[61] Jeney V, Balla J, Yachie A, Varga Z, Vercellotti GM, Eaton JW, et al. Pro-oxidant and cytotoxic effects of circulating heme. Blood 2002;100:879–87.